

Fatal Rhinoorbital Mucormycosis in a Child with Fanconi Anemia: The Critical Role of CT Imaging

Amal Akammar ^{1,*}, Younes Abdourabbih ¹, Hajar Ouazzani ¹, Ismail Chaouche ², Nizar El Bouardi ², Meriem Haloua ¹, Badreddine Alami ², Moulay Youssef Alaoui Lamrani ², Mustapha Maaroufi ² and Meryem Boubbou ¹

¹ Department of Radiology, Mother and Child hospital, CHU Hassan II, sidi Mohammed Ben Abdellah university, Fes, Morocco.

² Department of Radiology, CHU Hassan II, sidi Mohammed Ben Abdellah university, Fes, Morocco.

World Journal of Advanced Research and Reviews, 2026, 30(03), 048-052

Publication history: Received on 23 April 2026; revised on 29 May 2026; accepted on 01 June 2026

Article DOI: <https://doi.org/10.30574/wjarr.2026.30.3.1563>

Abstract

Mucormycosis is a severe, angioinvasive fungal infection associated with elevated mortality rates, particularly in immunocompromised patients. Rhinoorbital mucormycosis (ROM) is one of its most prevalent and fatal forms, typically manifesting with nonspecific sinonasal symptoms before rapidly advancing to orbital and intracranial complications. Prompt identification of subtle imaging signs is essential for early intervention. We present a case of rhinoorbital mucormycosis in a 10-year-old child with Fanconi anemia-associated bone marrow aplasia, emphasizing critical CT findings including obliteration of peri-antral fat, deep facial and masticator space involvement, extension through the sphenopalatine fissure and inferior orbital fissure, and progressive orbital proptosis. This case highlights the pivotal role of CT imaging in early extrasinus disease detection and the unique challenges of management in a severely thrombocytopenic pediatric patient in whom surgical debridement a cornerstone of treatment was formally contraindicated.

Keywords: Mucormycosis; Rhinoorbital mucormycosis; Acute invasive fungal rhinosinusitis; Fanconi anemia; Bone marrow aplasia; Immunocompromised child;

1. Introduction

Mucormycosis is a severe, opportunistic fungal infection caused by fungi of the order Mucorales, primarily affecting individuals with diabetes mellitus, hematological malignancies, immunosuppression, or conditions associated with elevated free serum iron levels [1,2]. Rhinoorbital mucormycosis is one of its most common and lethal clinical presentations, characterized by rapid progression from the nasal mucosa and paranasal sinuses to the orbit, skull base, and intracranial structures [1-3]. Initial clinical manifestations are frequently nonspecific, overlapping with those of common bacterial rhinosinusitis, which may delay diagnosis and worsen outcomes. In the immunocompromised pediatric host, this diagnostic challenge is further compounded by the attenuation of classical inflammatory signs, including the potential absence of osseous destruction on early imaging.

Cross-sectional imaging, particularly contrast-enhanced CT of the facial massif and orbits, plays an essential role in early disease suspicion, extent evaluation, identification of complications, and surgical planning [3-5,7,8]. Recognizing subtle but critical CT features such as peri-antral fat stranding, deep fascial space involvement, and early orbital extension is of paramount importance for prompt multidisciplinary intervention. We report a case of rhinoorbital mucormycosis in a severely immunocompromised child with Fanconi anemia-associated bone marrow aplasia, highlighting key CT

* Corresponding author: Amal Akammar

features that distinguish invasive fungal disease from uncomplicated sinusitis and illustrating the unique management challenges posed by profound thrombocytopenia.

2. Case presentation

A 10-year-old male patient was first evaluated at the age of 6 years, born of a second-degree consanguineous marriage, with no prior notable medical history. He presented with pallor and epistaxis evolving over four months. Physical examination revealed a hemorrhagic syndrome consisting of ecchymotic patches over both upper and lower limbs, without dysmorphic features, organomegaly, or lymphadenopathy. Weight was 17 kg (-1 SD) and height 113 cm (mean). Initial workup showed severe pancytopenia: Hb 4.1 g/dL, WBC 2,100/ μ L (PNN 309/ μ L), platelets 19,000/ μ L, with reticulocytes at 27,376/ μ L and no blasts. Viral serologies were negative for HIV, HBV, HCV, and EBV; CMV IgG was positive. Parvovirus B19 IgM was subsequently found positive. Bone marrow biopsy was performed and the patient was managed with red blood cell (RBC) and platelet transfusions. Following further workup including bone marrow biopsy review and genetic studies, a diagnosis of bone marrow aplasia in the context of Fanconi anemia was established.

Over the following four years, the patient was followed on an outpatient basis with repeated hospitalizations for transfusion support. He required multiple platelet concentrate (PC) and packed red blood cell (PRBC) transfusions due to persistent severe thrombocytopenia (platelets frequently at 1,000–15,000/ μ L) and anemia (Hb ranging between 6.7 and 9.9 g/dL). Hemorrhagic episodes included petechiae and ecchymoses over the trunk and limbs, mucosal bleeding (gingival hemorrhage, oral hemorrhagic bullae), epistaxis, conjunctival hemorrhage, and hematuria. Platelet availability was frequently limited, leading to delays in transfusion support.

At the age of 10, the patient was admitted for management of febrile pancytopenia. He presented on Day 1 with fever, profound pancytopenia (Hb 7–7.5 g/dL, platelets 1,000/ μ L, PNN 200/ μ L), and clinical signs of cervicofacial cellulitis. Blood cultures drawn around Day 2 later returned positive for a coagulase-negative *Staphylococcus*, for which broad-spectrum antibiotic therapy including ceftriaxone was initiated. Despite treatment, fever persisted through Day 8, and the hemorrhagic syndrome worsened with recurrence of gingival bleeding and cola-colored urine.

Given clinical deterioration, the patient was transferred to the Pediatric Intensive Care Unit (PICU) on Day 8. The clinical picture included sepsis with altered consciousness (GCS 14, somnolence), polypnea, sustained fever, and progressive worsening of right hemifacial and periorbital swelling. Infectious workup revealed markedly elevated inflammatory markers (CRP 318 mg/L, PCT 19 ng/mL, WBC 490/ μ L). The appearance of a blackish necrotic plaque on the hard palate, combined with the radiological findings, established the diagnosis of invasive rhinoorbital mucormycosis complicating the cervicofacial cellulitis.

Contrast-enhanced CT of the facial massif and orbits was performed upon PICU admission and served as the cornerstone of the initial radiological workup. CT demonstrated complete opacification of the right maxillary sinus in an "en cadre" pattern, with spontaneously slightly elevated attenuation of the sinus contents, suggestive of acute fungal sinusitis. Bilateral nasal fossae demonstrated hypodense fluid-like opacification, more pronounced on the right side, consistent with associated rhinosinusitis. A collection was identified within the right peri-antral fat, measuring approximately 30 × 25 × 20 mm (height × anteroposterior × transverse diameters), extending superiorly along the sphenopalatine fissure toward the infratemporal fossa and through the inferior orbital fissure into the extraconal and intraconal fat, laterally in direct contact with the lateral pterygoid muscle, and anteriorly abutting the anterior wall of the maxillary bone, without osseous lysis or periosteal reaction. This orbital extension was responsible for grade I proptosis. Extensive infiltration of the right jugal subcutaneous soft tissues and parapharyngeal fat was also noted, with diffuse enlargement and infiltration of the ipsilateral lateral pterygoid, masseter, and temporal muscles, consistent with direct myositis from contiguous fascial spread. The cerebral parenchyma showed no detectable abnormality, with no evidence of cerebral abscess, hemorrhagic infarction, cavernous sinus thrombosis, leptomeningeal enhancement, or cerebral edema (Figure 1).

Antifungal therapy was initiated on Day 8 with liposomal amphotericin B (AmBisome) at 3 mg/kg/day (75 mg/day), diluted in 5% glucose and administered over at least 2 hours. Broad-spectrum antibacterial coverage was maintained with imipenem-cilastatin every 6 hours and teicoplanin once daily. Supportive care included paracetamol, esomeprazole, parenteral nutrition (SMOFkabiven, progressively increased to 90% of Schofield requirements), and nasogastric tube feeding. Topical ocular treatments were added, including tobramycin eye drops, sodium hyaluronate/trehalose lubricant drops, and dexpanthenol ophthalmic gel, alongside systemic hypotonic therapy (Xolamol 1 tablet twice daily) prescribed by the ophthalmology team. Surgical debridement, though indicated as a cornerstone of mucormycosis management, was formally contraindicated throughout the entire PICU course due to severe thrombocytopenia (persistent platelet count of 1,000/ μ L).

Hemodynamically, the patient remained relatively stable during the early PICU course, with blood pressure around 120/50 mmHg and preserved diuresis, not initially requiring vasopressor support. He exhibited persistent tachycardia (heart rate 120–175 bpm), attributed to the combination of fever, anemia, hypokalemia (as low as 2.6 mEq/L), and hypomagnesemia (as low as 12 mg/L), both corrected with repeated electrolyte supplementation. Neurologically, consciousness gradually deteriorated (GCS 14, somnolence) without focal sensorimotor deficit or seizures. Hematologically, transfusion dependence continued with persistent non-correctable thrombocytopenia (1,000/ μ L) and progressive anemia (Hb declining to 4.8–5.5 g/dL). On Day 16, hemodynamic instability emerged requiring initiation of norepinephrine at 1.5 μ g/kg/min, adjusted continuously to hemodynamic status. Despite transient stabilization under maximal supportive care and ongoing antifungal therapy, the patient developed progressive respiratory distress and refractory septic shock, which ultimately proved fatal.

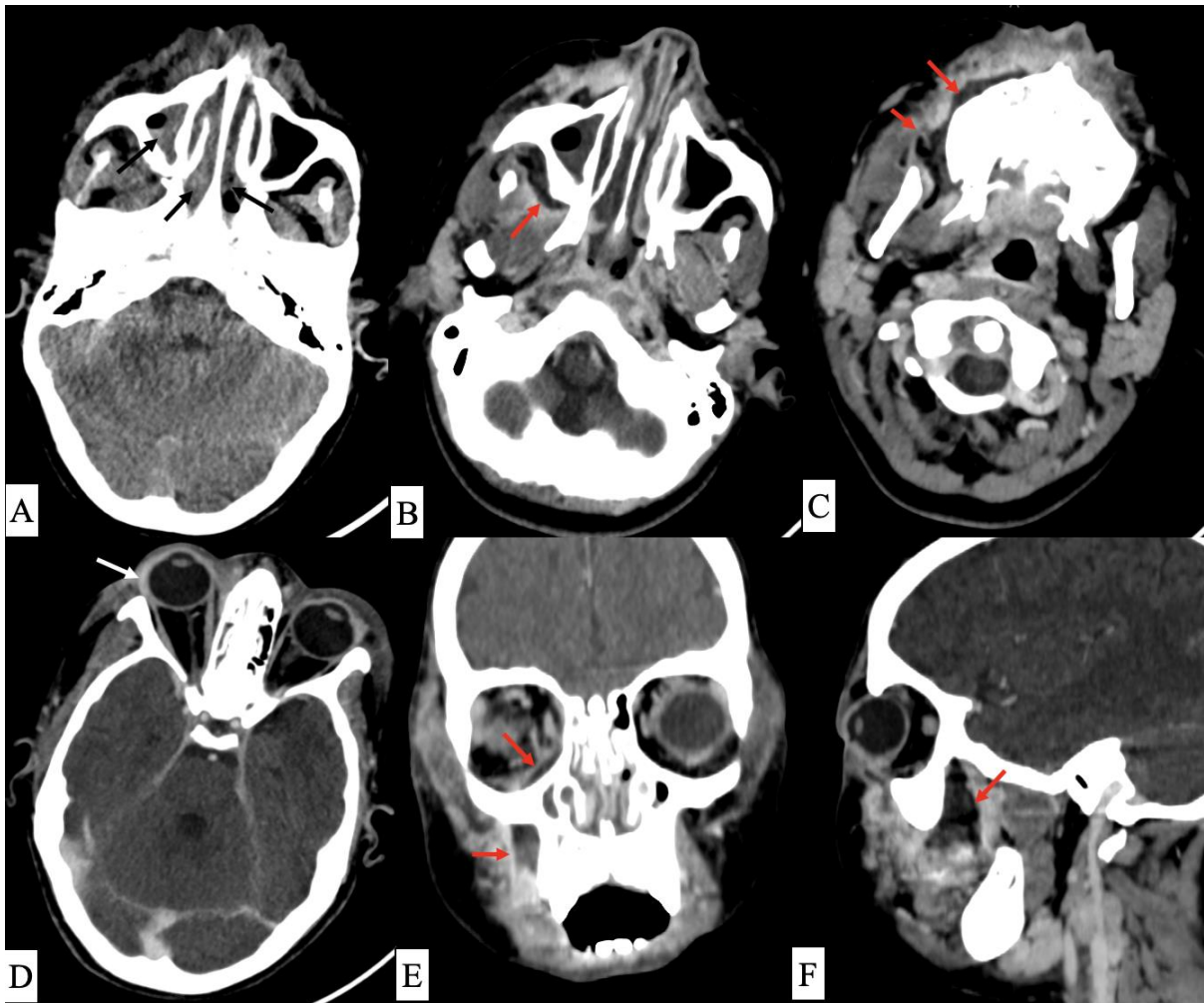


Figure 1 Contrast-enhanced CT of the facial massif and orbits. (A) Axial CT showing complete right maxillary sinus opacification in an "rim-like" pattern with spontaneously slightly elevated attenuation (black arrows), associated with bilateral nasal fossae fluid-like opacification. (B) Axial CT showing the right peri-antral collection extending into the infratemporal fossa along the sphenopalatine fissure (red arrow). (C) Axial CT demonstrating infiltration of the masticator space with enlargement of the ipsilateral masseter and temporal muscles (red arrows), consistent with direct myositis from contiguous fascial spread. (D) Axial CT at the orbital level showing right extraconal fat infiltration responsible for grade I proptosis (white arrow), without osseous lysis. (E) Coronal reconstruction demonstrating the right maxillary sinus opacification with superior extension of the collection through the inferior orbital fissure into the right orbital fat (red arrows). (F) Sagittal reconstruction showing the craniocaudal extent of the collection along the sphenopalatine fissure without periosteal reaction or cortical erosion (red arrow). No intracranial abnormality was identified on any of the acquired sequences

3. Discussion

Mucormycosis is a severe, angioinvasive fungal infection caused by organisms of the order Mucorales, carrying significant mortality, particularly in immunocompromised hosts such as patients with hematological malignancies, prolonged neutropenia, or aplastic anemia [1,2]. Unlike the most commonly reported risk factor of uncontrolled diabetes mellitus, the present case illustrates the equally lethal potential of mucormycosis in a pediatric patient with Fanconi anemia-associated bone marrow aplasia, a clinical context associated with profound and refractory pancytopenia that severely limits both host immune response and therapeutic options.

Rhinoorbital mucormycosis generally originates in the nasal mucosa and paranasal sinuses, initially manifesting with nonspecific symptoms including fever, facial pain, nasal congestion, and discharge. However, it can progress rapidly within hours to days to orbital involvement and, in advanced cases, to skull base and intracranial extension, necessitating a high index of suspicion and prompt cross-sectional imaging [1,3,4]. In neutropenic patients, the classical hallmark of osseous destruction may be absent or delayed, as the local inflammatory response responsible for bone resorption is impaired, making early soft tissue and fat plane changes even more critical radiological targets.

Computed tomography remains the first-line imaging modality in suspected rhinoorbital mucormycosis, owing to its speed, wide availability, and ability to depict both sinonasal disease and extrasinus involvement [3–5,7]. Key early CT findings include disproportionately dense or heterogeneous sinus opacification, infiltration or replacement of peri- and retro-antral fat, and subtle extrasinus soft tissue changes all of which may precede overt osseous destruction. In our case, the spontaneously elevated attenuation of right maxillary sinus contents and the peri-antral collection with multidirectional fascial spread through the sphenopalatine fissure, infratemporal fossa, and inferior orbital fissure represented the cardinal CT features of invasive fungal sinusitis, even in the absence of bony lysis [3–5,7].

A defining characteristic of mucormycosis is its propensity for angioinvasion and perivascular spread, enabling transgression of intact bony barriers. Orbital involvement, which may occur through the lamina papyracea, nasolacrimal duct, or via the pterygopalatine and inferior orbital fissures as observed in this case is a critical determinant of visual and overall outcomes [1,3,4]. It manifests as orbital fat stranding, extraocular muscle thickening, proptosis, and, in advanced stages, orbital apex infiltration.

MRI with gadolinium enhancement and diffusion-weighted imaging (DWI) would have provided superior evaluation of perineural spread, early cavernous sinus involvement, and ischemic parenchymal changes secondary to vascular invasion features that CT may underestimate [3–5]. The "black turbinate" sign on post-contrast MRI, characterized by non-enhancing turbinate mucosa reflecting ischemic necrosis, represents a strongly suggestive early marker of ROCM [5,6].

The management of mucormycosis requires a prompt, multimodal approach combining aggressive antifungal therapy and surgical debridement [1–4,7,8]. Liposomal amphotericin B at 5–10 mg/kg/day is the recommended first-line antifungal agent in children, with a minimum treatment duration of twelve weeks [9]. In our patient, antifungal therapy was initiated at 3 mg/kg/day at the lower end of the recommended range reflecting the limited local drug supply. Critically, surgical debridement, which is essential for disease control by removing necrotic tissue that antifungals cannot adequately penetrate due to angioinvasion-related vascular compromise, was formally contraindicated throughout the course due to persistent severe thrombocytopenia. This represents a therapeutic impasse unique to hematological patients and a major contributor to the fatal outcome in this case.

4. Conclusion

This case demonstrates that rhinoorbital mucormycosis in a severely immunocompromised pediatric patient can be suspected at an early stage through careful interpretation of CT findings, even in the absence of the classical hallmark of osseous destruction. Peri-antral fat obliteration, multidirectional fascial spread through the sphenopalatine fissure and inferior orbital fissure, deep masticator space myositis, and progressive orbital proptosis were the critical imaging indicators that established the diagnosis and guided management. Radiologists play a pivotal role in fostering early suspicion, delineating disease extent, and alerting the multidisciplinary team for prompt intervention. In hematological patients with refractory thrombocytopenia, the inability to perform surgical debridement represents a unique and often insurmountable therapeutic challenge, underscoring the critical importance of early antifungal therapy and the need to optimize drug dosing within recommended ranges from the outset.

Compliance with ethical standards

Disclosure of conflict of interest

No conflict of interest to be disclosed.

Statement of informed consent

Informed consent was obtained from all individual participants included in the study.

References

- [1] Spellberg B, Edwards J Jr, Ibrahim A. Novel perspectives on mucormycosis: pathophysiology, presentation, and management. *Clin Microbiol Rev.* 2005;18(3):556–569.
- [2] Roden MM, Zaoutis TE, Buchanan WL, et al. Epidemiology and outcome of zygomycosis: a review of 929 reported cases. *Clin Infect Dis.* 2005;41(5):634–653.
- [3] Therakathu J, Prabhu S, Irodi A, et al. Imaging features of rhinocerebral mucormycosis: a study of 43 patients. *Egypt J Radiol Nucl Med.* 2018;49(2):447–452.
- [4] Aribandi M, McCoy VA, Bazan C 3rd. Imaging features of invasive and noninvasive fungal sinusitis: a review. *Radiographics.* 2007;27(5):1283–1296.
- [5] Safder S, Carpenter JS, Roberts TD, Bailey N. The "black turbinate" sign: an early MR imaging finding of nasal mucormycosis. *AJNR Am J Neuroradiol.* 2010;31(4):771–774.
- [6] Nair AG, Dave TV, Trans Mucor Study Group, et al. Defining the 'black turbinate' sign on MRI in COVID-19-associated rhino orbito cerebral mucormycosis. *Clin Neuroradiol.* 2022;32(1):199–206.
- [7] Middlebrooks EH, Frost CJ, De Jesus RO, et al. Acute invasive fungal rhinosinusitis: a comprehensive update of CT findings and design of an effective diagnostic imaging model. *AJNR Am J Neuroradiol.* 2015;36(8):1529–1535.
- [8] Chikermane A, Nair AG, Dave TV, et al. Imaging of COVID-19-associated rhino orbito cerebral mucormycosis: a multicentric study. *Indian J Ophthalmol.* 2021;69(7):1915–1927.
- [9] Alby-Laurent F, et al. Infections fongiques invasives chez l'enfant immunodéprimé en hématologie pédiatrique : recommandations de prise en charge au sein des centres de la SFCE. *Bull Cancer.* 2022;109:1109–1124.